

FIG. 2. Sample in the form of a pile of identically oriented bismuth disks (4), with a copper disk (3); an inductance coil creating a low-frequency alternating field is denoted by 2 and measuring inductance coils are denoted by 1.

In the second case the measurements were made using a pile identically oriented bismuth disks (Fig. 2). A narrow gap at the center of a pile contained two planar coaxial inductance coils. The largest diameters of these coils were $2r_2 = 4$ mm and $2r_1 = 12$ mm. The width of each coil a was 1 mm. A recording system similar to that shown in Fig. 1 plotted the voltage across one of these measuring coils as a function of the phase of the current flowing through a superconducting driving inductance coil. The pile of disks consisted of six bismuth samples. The edge effects were determined by making a series of measurements on a pile of disks covered above and below by two copper disks of the same diameter and 2 mm thick (as shown in Fig. 2), and then the measurements were repeated on the pile of bismuth without the copper disks. The agreement between the two sets of results demonstrated that the edge effects were unimportant.

Typical records obtained from the measuring coils inside the pile of disks are plotted in Fig. 3. It is clear from this figure that the variation of the magnetic flux in the interior of the sample was nonsinusoidal. The experimental curves could easily be interpreted assuming that the magnetic field penetrated in the nonlinear regime into the semimetal as a wave with a sharp front. The magnetic field had opposite signs on the two sides of the front. The section AB in Fig. 3 represents the passage of the wave front through the circular windings of one of the measuring coils, whereas at the point A' the front reaches the second measuring coil, and the point

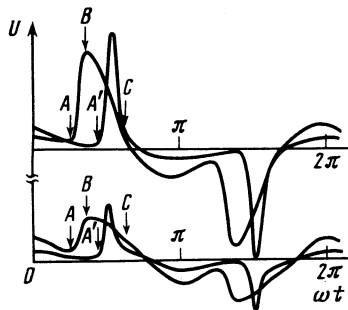


FIG. 3. Examples of records of a signal obtained from the measuring coils. The upper curves correspond to $\omega/2\pi = 10^3$ Hz and $H_0 = 66$ Oe. The lower curves correspond to $\omega/2\pi = 170$ Hz and $H_0 = 40$ Oe.

C corresponds to the collapse of the wave at the center of the sample. The wave was generated on the surface of the metal at those moments when the magnetic field on the surface reversed its sign and traveled a distance of the order of the radius of the sample (9 mm) without strong damping. In the linear regime the skin layer depth measured in the same experiment was 1.1 ± 0.1 mm at the frequency of 10^3 Hz.

Records similar to those shown in Fig. 1 allowed us to calculate readily the velocity V of the wave front and to estimate the front width. The average velocity of the wave in the gap between the radii of the measuring coils r_1 and r_2 was found by dividing the distance $r_1 - r_2$ by the time interval $\Delta t(AA')$ in which the wave traversed this gap. The width b of the wave front is given by

$$b = V\Delta t(AB) - a.$$

The dependence of the wave propagation velocity on the amplitude of the field on the surface of a sample and on the wave frequency are plotted in Fig. 4. At the frequency of $\omega/2\pi = 170$ Hz the width of the front was within the range 1 – 1.5 mm and it depended weakly on the amplitude of the alternating field at the boundary of the semimetal when the amplitude was increased from 30 to 300 Oe. Reduction of the field amplitude below 30 Oe broadened the wave front. The presence of a sharp front in which the magnetic field sign changed corresponded to a peak of the current traveling into the sample.

A typical experimental curve obtained in measurements on a single disk placed inside a planar (rectangular) inductance coil is plotted in Fig. 5. It is clear from this figure that the derivative of the magnetic flux through the sample $\partial\Phi/\partial t$ exhibited not only a signal at the first harmonic (eliminated mainly by the bridge circuit), but also sharp singularities at the moments when the magnetic field on the sample surface vanished. An increase of the frequency at a fixed amplitude of the alternating field increased the line width φ (Fig. 5) as shown in Fig. 6a. The dependence of φ on the alternating field amplitude had the form shown in Fig. 6b. The line amplitude J rose linearly on increase in the alternating field intensity. Slight deviations from the linear dependence (Fig. 7a) were observed only at low intensities of the alternating field at the lowest frequency $\omega/2\pi = 150$ Hz used in our experiments. An increase in the frequency at a fixed amplitude of the alternating field resulted in a linear (within the limits of the experimental error) increase in the line amplitude (Fig. 7b).

DISCUSSION

We shall consider the penetration of a large-amplitude low-frequency alternating field into a compensated metal using, as in Ref. 7, the local coupling between the field and current which can be regarded as a rough approximation:

$$j = \sigma E, \quad \sigma = \sigma_0 / [1 + (\omega_c \tau)^2], \quad (2)$$

where σ is the transverse static conductivity; $\omega_c = eH/mc$ is the cyclotron frequency; σ_0 is the conductivity of the metal in the absence of a magnetic field. It is assumed that the transverse conductivity σ depends on the magnetic field H of

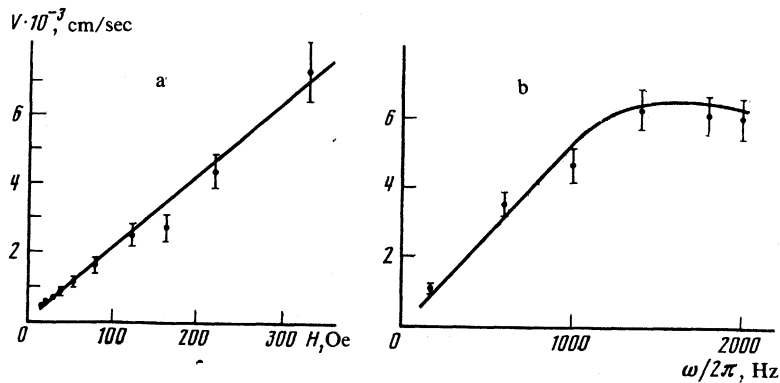


FIG. 4. Dependences of the velocity of the wave front: a) on the amplitude of an alternating field on the surface of the semimetal $\omega/2\pi = 170$ Hz; b) on the frequency of an alternating field of amplitude $H_0 = 55$ Oe.

the wave in the same way as on a homogeneous external magnetic field.

We shall consider the penetration of a wave in a plate of thickness d oriented in the xy plane and we shall assume that on the surface of the plate an alternating magnetic field $\mathbf{H}||x$ varies sinusoidally.

$$H(-d/2, t) = H(d/2, t) = H_0 \sin \omega t.$$

We shall introduce dimensionless quantities: $u = H\alpha^{1/2}$, where $\alpha = (\omega_c \tau / H)^2$; $\xi = z/\delta_0$, where $\delta_0 = (c^2 / 4\pi\sigma_0\omega)^{1/2} = \delta/\sqrt{2}$; $t_1 = \omega t$, $\xi_0 = d/\delta_0$, $U_0 = H_0\alpha^{1/2}$. Eliminating the electric field from the Maxwell equations, we obtain

$$\frac{\partial}{\partial \xi} \left\{ (1+u^2) \frac{\partial u}{\partial \xi} \right\} = \frac{\partial u}{\partial t_1}. \quad (3)$$

This equation is analogous to the diffusion equation with a concentration-dependent diffusion coefficient.

We solved numerically Eq. (3) for a number of cases. In a comparison of the results of this numerical calculation with the experimental data it was essential to know the parameter $\alpha^{-1/2}$. This parameter was determined separately from the dependence of the skin layer depth in the linear regime on a static external magnetic field. At 4.2°K the value of $\alpha^{-1/2}$ was 6 Oe.

By way of a typical example, Fig. 8 shows the distribution of the magnetic field across the bulk of a sample in the case of a thick plate $\xi_0 = 30$. It is clear from Fig. 8 that the magnetic field penetrates to a distance considerably greater than δ_0 and the greatest change in the magnetic field occurs in the region where $u \leq 1$. The wave penetrating into the sample does not have a sharp front because a significant change in the magnetic field occurs over distances which are much greater than δ_0 . The maximum of the electric field of

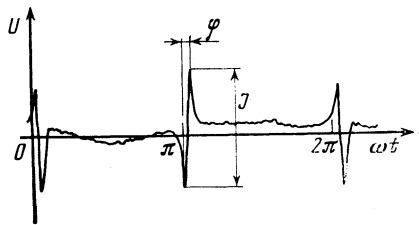


FIG. 5. Experimental record of a signal obtained for a thin sample at $T = 4.2$ °K for $\omega/2\pi = 155$ Hz and $H_0 = 220$ Oe.

the wave lies in the vicinity of the points corresponding to $u = 0$.

The point $u = 0$ travels rapidly into a sample. The velocity of this point corresponding to $U_0 = 20$ remains practically constant in the interval $1 \leq \xi \leq 20$ and it amounts to $V = 66\delta\omega/2\pi$ cm/sec. A similar dependence, but with a different numerical coefficient and in a different range of ξ , is obtained for other values of the alternating field amplitude on the surface of a sample. The calculated dependence of the wave front velocity on the frequency $V \propto \omega^{1/2}$ does not agree with the experimental results (Fig. 4b).

A signal recorded in measurements on a pile of disks is proportional to the electric field at a distance $z_1 = (D - 2r_1)/2$ from the surface of the sample. A direct comparison with the experimental curves was made by calculating the time dependence of $E(z_1)$ for a plate of thickness $\xi_0 = D/\delta_0$. The results of this calculation and the corresponding experimental curve are plotted in Fig. 9. The rise of the electric field (section AB) observed experimentally occurred in a shorter time interval than that expected from the calculation. (One should bear in mind that only broadening of the observed curve could be expected because of the finite width of the measuring coil and some noncoaxiality of its position.)

A more rapid rise of the electric field corresponds to a more abrupt front of the wave penetrating the sample. Consequently, the relationships (2) and (3) underestimate the density of the current in the vicinity of those points in the sample at which the magnetic field of the wave changes its sign.

We shall now consider the experiments carried out on the same bismuth disk. Then, using the relationship (2) between the electric field and the current at the lowest of the experimental frequencies (170 Hz), we can regard the thickness of the sample as small compared with the skin-layer depth ($\xi_0/2 \ll 1$) and solve Eq. (3) by the method of successive approximation:

$$\frac{\partial}{\partial \xi} \left\{ (1+u_k^2) \frac{\partial u_k}{\partial \xi} \right\} = \frac{\partial u_{k-1}}{\partial t_1}, \quad (4)$$

$$u_k(-\xi_0/2, t_1) = u_k(\xi_0/2, t_1) = U_0 \sin t_1 = u_0(\xi, t_1).$$

In the first approximation, we find from Eq. (4) that

$$u_1(\xi, t_1) + \frac{1}{3}u_1^3(\xi, t_1) = -\frac{1}{2}U_0 \cos t_1 \left(\frac{\xi_0^2}{4} - \xi^2 \right) + U_0 \sin t_1 + \frac{1}{3}U_0^3 \sin^3 t_1. \quad (5)$$

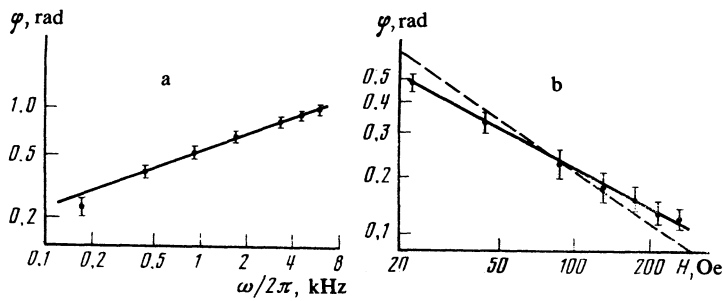


FIG. 6. Dependences of the line width: a) on the frequency of an alternating field of $H_0 = 88$ Oe amplitude (the straight line corresponds to the dependence $\varphi \propto \omega^{1/3}$); b) on the amplitude of an alternating field of $\omega/2\pi = 160$ Hz frequency (the dashed curve corresponds to the dependence $\varphi \propto H^{-2/3}$ and the continuous one to $\varphi \propto H^{-1/2}$).

The experimentally recorded quantity is proportional to

$$U \propto \frac{\omega \delta}{\alpha^{3/4}} \frac{\partial}{\partial t_1} \int_0^{\xi_0/2} \{u_1(\xi, t_1) - U_0 \sin t_1\} d\xi. \quad (6)$$

It follows from Eqs. (5) and (6) that in the case corresponding to the experimental situation ($U_0 > 8\xi_0^2$) we can readily obtain the dependences of the width and amplitude of the experimentally observed lines on the intensity and frequency of the alternating field:

$$\varphi \propto \omega^{1/4} / H_0^{3/4}, \quad J = U_{max} - U_{min} \propto H_0 \omega d. \quad (7)$$

The dependence of the amplitude of the experimentally observed lines on the magnetic field intensity (Fig. 7b) and frequency (Fig. 7a), like the dependence of the line width on the alternating frequency (Fig. 6), are in agreement—within the limits of the experimental error—with the calculations based on the formulas in Eq. (7). However, the variation of the line width with increase in the alternating field intensity does not agree with the calculations. Moreover, the agreement with the experimental results is obtained for the dependences observed at those frequencies (2–6 kHz) which correspond to $\xi_0/2 \gtrsim 1$ and where the above solution is invalid. Therefore, we should regard the agreement between some of the calculated dependences and the experimental data as purely accidental.

The obvious reason for the discrepancy between the calculations and experiments is an inhomogeneity of the magnetic field of the wave. In an inhomogeneous field with a alternating sign it is found that a layer of twisted trajectories (Fig. 10) is observed near the surface at which the magnetic field of the wave reverses sign; these trajectories are similar

to those which are responsible for the appearance of current states in metals.^{3,8} The distance traveled, in the direction of the electric field, by electrons moving along such trajectories is of the same order of magnitude as the mean free path. We shall now consider under what conditions the presence of a layer of twisted trajectories may be important for the formation of the front of an electromagnetic wave in a compensated metal. We shall assume that the magnetic field of the wave has the components $H_x = Bz$ and $H_y = H_z = 0$. The distance z_0 traveled by an electron from the surface $H = 0$ is readily found from the condition

$$P_y + \frac{e}{c} A_y = P_y + \frac{e}{c} \int_0^{z_0} Bz dz = P_y + \frac{e}{c} \frac{B}{2} z_0^2 = \text{const.} \quad (8)$$

The order of magnitude of the width of the layer of the twisted trajectories of interest to us agrees with the maximum distance traveled from the $H = 0$ surface by electrons crossing this surface:

$$z_0 \propto (pc/eB)^{1/2}. \quad (9)$$

At distances $z < z_0$ the electric current is governed by the average value of the electric field, i.e., the coupling between the field and current is nonlocal. The effective conductivity at these distances is of the same order of magnitude as the conductivity of a metal in the absence of a magnetic field.

The presence of a layer of twisted trajectories alters significantly the distribution of the fields and currents compared with that given by Eqs. (2) and (3), if the magnetic field at a distance z_0 from the $H = 0$ surface is strong:

$$\alpha^{1/2} H(z_0) = eBz_0 \tau / mc \gg 1, \quad \text{or} \quad B = \partial H / \partial z (z=0) \gg pc / e\tau^2. \quad (10)$$

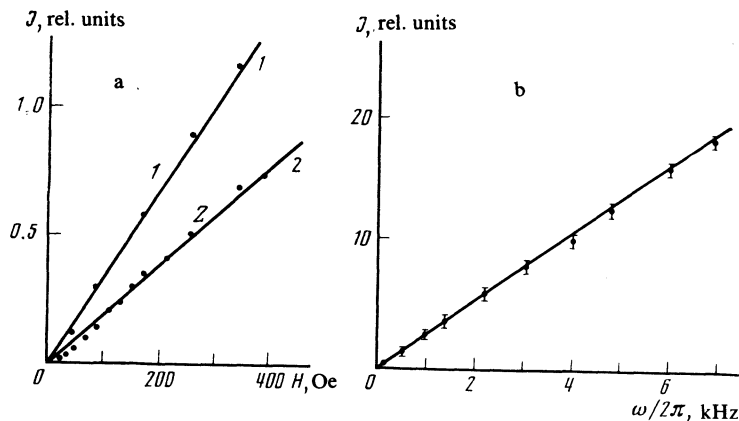


FIG. 7. Dependences of the line amplitude J on: a) the amplitude of an alternating field (line 1 represents $J/10$ at a frequency $\omega/2\pi = 2.6 \times 10^3$ Hz, whereas 2 is the line amplitude at $\omega/2\pi = 150$ Hz); b) the frequency of an alternating field of $H_0 = 220$ Oe amplitude.

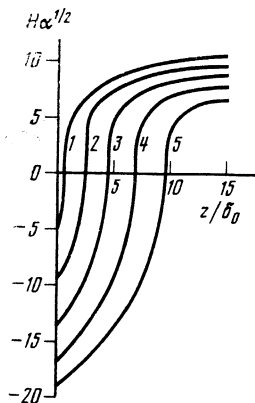


FIG. 8. Results of a calculation of the distribution of a magnetic field in the bulk of a sample carried out for different phases of the field on the surface. The dimensionless amplitude of the alternating field is assumed to be $U_0 = 20$ on the surface. Curve 1 corresponds to an alternating field phase $\omega t = 8\pi/100$; 2) $\omega t = 16\pi/100$; 3) $\omega t = 24\pi/100$; 4) $\omega t = 32\pi/100$; 5) $\omega t = 40\pi/100$.

Under the conditions of the normal skin effect the magnetic field gradient of a damped electromagnetic wave of amplitude H_0 is of the order of H_0/δ . If we assume that the magnetic field gradient is of the same order of magnitude also under nonlinear conditions, we then obtain the condition (1) from Eq. (10).

In an inhomogeneous magnetic field the trajectories of all electrons are not closed (Fig. 10). Each of the electrons travels along the electric field of the wave. The distance traveled between two scattering events is governed by the dependence of the magnetic field on the coordinates. In the simplest case, we have

$$H(z) = H(z_1) + B(z - z_1).$$

If the charge in the magnetic field intensity over a characteristic dimension of an electron trajectory $r_0 = pc/eH(z_1)$ is slight, i.e., if

$$H(z_1) \gg (Bpc/e)^{1/2}, \quad (11)$$

the displacement of an electron parallel to the electric field in a time τ is

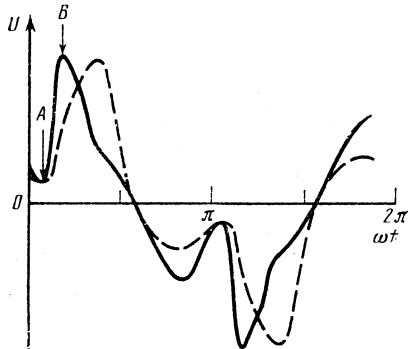


FIG. 9. Comparison of the experimentally observed signal (continuous curve) with the calculated one (dashed curve). The scale of the calculated curve along the ordinate is selected so that the maximum value of U agreed with the experimental value. $U_0 = 10$, $\omega/2\pi = 170$ Hz.

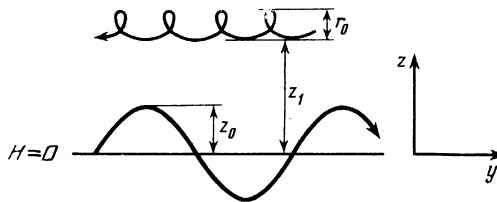


FIG. 10. Different types of electron trajectories in an inhomogeneous magnetic field. This field is parallel to the x axis and it changes its sign on the $z = 0$ plane.

$$\Delta y \sim BH^{-1}(z_1) (pc/eH(z_1))L. \quad (12)$$

The contribution of an electron to the conductivity changes significantly due to drift in an inhomogeneous magnetic field if the electron displacement Δy is greater than the electron orbit radius:

$$\Delta y \gg r_0 = pc/eH(z),$$

or

$$Bl \gg H(z_1). \quad (13)$$

Equations (11) and (13) give again the conditions (2) and (10) for the gradient of the magnetic field of a wave and for the amplitude of an alternating field on the surface of a sample.

It follows that in the case of sufficiently large amplitudes of an electromagnetic wave incident on the surface of a compensated metal the magnitude of the screening currents in the region where the magnetic field gradient is high depends not only on the values of E and H , but also on the magnetic field gradient. The relationship between the electric field and current in the vicinity of the points where $H = 0$ then becomes nonlocal and the equation describing the process of penetration of an electromagnetic field into the bulk of a metal cannot be reduced to an equation of the diffusion type. An increase in the effective conductivity in the region of rapid variation of the magnetic field intensity contracts the front of a wave traveling into the metal. It is this front narrowing that accounts for the faster (compared with the calculated) rise of the electric field with time in experiments on a pile of disks. If the width of the wave front is less than the penetration depth δ_0 , then a calculation carried out by the method of successive approximations to Eq. (4) is invalid. Therefore, the disagreement of the experimental dependence of $\varphi(H)$ obtained for a thin sample with the calculations also indicates contraction of the wave front and it supports the nondiffusion process of penetration of a large-amplitude low-frequency electromagnetic field into the interior of bismuth.

We shall conclude by noting that the nondiffusion nature of penetration of a low-frequency alternating field into the bulk of a metal should be observed in any compensated metal at low temperatures if the amplitude of the incident electromagnetic wave is sufficiently high.

The authors are deeply grateful to V. F. Gantmakher, L. M. Fisher, and I. F. Voloshin for numerous valuable discussions, and to Yu. P. Boglaev and R. R. Ponomareva for their help in the numerical calculations.

- ¹V. F. Gantmakher, G. I. Leviev, and M. R. Trunin, *Zh. Eksp. Teor. Fiz.* **82**, 1607 (1982) [*Sov. Phys. JETP* **55**, 931 (1982)].
- ²E. G. Yashchin, *Fiz. Tverd. Tela (Leningrad)* **22**, 2293 (1980) [*Sov. Phys. Solid State* **22**, 1335 (1980)].
- ³V. T. Dolgoplov, *Usp. Fiz. Nauk* **130**, 241 (1980) [*Sov. Phys. Usp.* **23**, 134 (1980)].
- ⁴V. T. Dolgoplov, S. S. Murzin, and P. N. Chuprov, *Zh. Eksp. Teor. Fiz.* **78**, 331 (1980) [*Sov. Phys. JETP* **51**, 166 (1980)].
- ⁵V. V. Boiko, L. V. Ovchinnikova, and G. N. Landysheva, *Pis'ma Zh.*

- Eksp. Teor. Fiz.* **32**, 432 (1980) [*JETP Lett.* **32**, 408 (1980)].
- ⁶V. I. Bozhko and E. P. Vol'skiĭ, *Zh. Eksp. Teor. Fiz.* **72**, 257 (1977) [*Sov. Phys. JETP* **45**, 135 (1977)].
- ⁷V. V. Vas'kin, I. F. Voloshin, V. Ya. Demikhovskii, and L. M. Fisher, *Fiz. Nizk. Temp.* **5**, 605 (1979) [*Sov. J. Low Temp. Phys.* **5**, 289 (1979)].
- ⁸N. M. Makarov and V. A. Yampol'skiĭ, *Pis'ma Zh. Eksp. Teor. Fiz.* **35**, 421 (1982) [*JETP Lett.* **35**, 520 (1982)].

Translated by A. Tybulewicz